(32) Hsu, C. S.; Percec, V. *J. Polymn. Sci., Part A: Polym. Chem. Ed.* 1987, *25*, 2909.
(33) Kwolek, S. L.; Luise, R. R. *Macromolecules* 1986, *19*, 1789.

Pattabiraman Balakrishnan* and Issifu I. Harruna
Department of Chemistry, Atlanta University
Atlanta, Georgia 30314

Malcolm B. Polk*
School of Textile Engineering & Polymer Group
Georgia Institute of Technology
Atlanta, Georgia 30332

Received August 11, 1987

Determination of the Chain Conformation in Fast-Spun Polypropylene Fibers by Small-Angle Neutron Scattering†

In the melt spinning process filaments (fibers) are formed by extruding a polymer melt through a capillary and simultaneously applying an extensional force to the extrudate. The filaments are taken up by a winder with a constant take-up velocity. Along the spinning path the fluid extrudate is deformed, cooled, solidified, and transformed into a filament with a highly anisotropic supramolecular structure. For crystalline polymers such as polypropylene (PP), it is well-known[1-3] that for sufficiently high take-up velocities, the solidification along the spinning line is due to a stress-induced crystallization process. For fast spun fibers Vassilatos et al.[4] suggested that the crystallization takes place in the highly oriented, affinely deformed melt. One of the interesting questions with respect to such an orientation-induced crystallization process is the way a single molecular chain is incorporated into the semicrystalline structure of the fiber.

Small-angle neutron scattering (SANS) on deuterium labeled molecules, dissolved in a nondeuterated matrix, is the ideal tool to investigate this problem. Scattering experiments yield the scattering form factor of a single labeled molecule and, therefore, its morphology. This report gives first results of such scattering experiments on fast-spun fibers, spun from a blend of perdeuteriated PP and nondeuteriated PP, for two take-up velocities.

As Ziabicki[3-5] has shown, the stress σ_s at the solidification point is strongly dependent on the take-up velocity v_a. In the velocity range considered in our experiments, the relation $\sigma_s = \text{const} \times v_a^2$ is valid to a good approximation. Consequently, the take-up velocity is expected to influence strongly the morphology; as will be shown, this cannot be concluded from our measurements. For comparison, we have also investigated fibers spun, without take-up, and mechanically cold-drawn by a necking process.

Experiments. As nondeuteriated matrix material, a degraded isotactic homo-PP has been used with a molecular mass M_w = 210 000 g/mol and M_w/M_n = 2. The perdeuteriated material was prepared in a 1000-cm^3 autoclave by using a gas-phase polymerization technique. A normal Ziegler catalyst was used. Experience shows that with the procedure used, a value M_w/M_n of about 7 is obtained. In view of the great amount of PP-*d* sample material required (1 kg for each deuterium concentration studied!) a fractionation has not been performed. D6-Propen was bought from IC-Chemicals. The molecular mass was M_η = 130 000 g/mol as determined by viscosimetry. The deuteriated and nondeuteriated PP were mixed mechanically. In order to achieve a homogeneous distribution of the components the mixture was extruded twice at 200 ± 5 °C. Fibers with two concentrations of the perdeuteriated material, c_D = 0.5% and 1.9%, were spun at take-up velocities v_a = 2500 and 4000 m/min. For each velocity, a nondeuteriated fiber was spun as a reference. In addition, samples with c_D = 0%, 0.5%, and 1.9% were extruded without applying an extensional force and afterward slowly cold-drawn by a necking process; the macroscopic draw ratio was λ = 4.

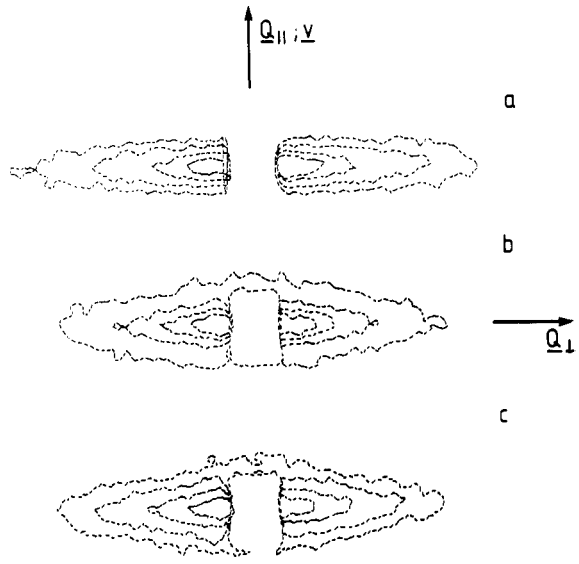

Figure 1. Contour plots for neutron small-angle scattering on polypropylene fibers (c_D = 1.9%): (a) cold-drawn sample; (b) fast-spun sample with take-up velocity v_a = 2500 m/min; (c) take-up velocity v_a = 4000 m/min. The fiber axis is parallel to the vertical axis in the diagrams.

The small-angle scattering experiments were carried out by using the diffractometer D 17 at the high-flux reactor in the ILL Grenoble. The wavelength was λ = 1.2 nm and the range of scattering vectors 0.09 nm$^{-1} \le Q \le$ 0.6 nm^{-1}, with $Q = (4\pi/\lambda) \sin\theta/2$ (θ = scattering angle). Figure 1 shows typical contour plots for the sample, cold-drawn by a necking process, and for the two fast-spun samples. The pictures demonstrate the elongation of the labeled molecules in the stretching direction: The meridional width of the intensity profile (parallel to the fiber axis) is so narrow that it disappears in the primary beam spot. The longitudinal extension of the contours is caused by the strongly reduced lateral dimension of the molecules.

For the further evaluation we used the radially averaged equatorial data; they were integrated over sectors with a half-width of 22.5°. The incoherent scattering background for all samples was individually determined by using the meridional intensities at large Q, where the coherent scattering has practically decayed to zero. After subtraction of the incoherent background, the coherent intensities were normalized by the measured sample transmission. In order to correct for the different sample volumes, these scattering intensities were finally normalized by means of the measured incoherent scattering of the samples. This procedure introduces uncertainties as high as 20% caused by irregularities in the packing density of the sample coils.

Parasitic coherent scattering at small Q was corrected for by subtracting the coherent scattering of the corresponding unlabeled samples. In each case the coherent scattering from the unlabeled samples was less than 20% of the scattering from the labeled samples. Under these conditions, the above-mentioned uncertainties with respect to the scattering volume should not lead to significant errors as concerns the correction for parasitic coherent scattering. A comparison of the corrected data for c_D =

† Dedicated to Professor Dr. Helmut Dörfel on the occasion of his 60th birthday.

0024-9297/88/2221-1541$01.50/0

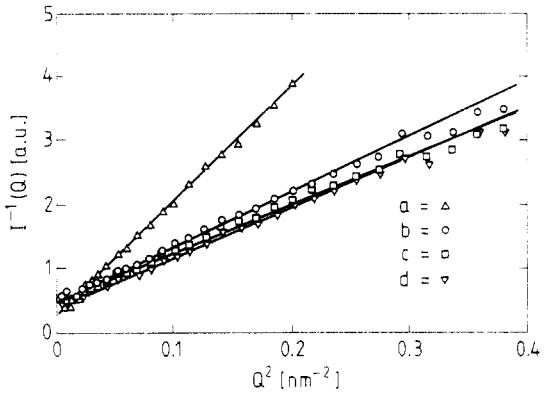

Figure 2. Corrected scattering data plotted in the Zimm representation for the samples: (a) spun with no take-up; (b) spun with v_a = 2500 m/min; (c) spun with v_a = 4000 m/min; (d) spun with no take-up and cold-stretched (arbitrary units, not normalized).

Table I
Radius of Gyration $\langle R_g^2\rangle^{1/2}$, $\langle R_\perp^2\rangle^{1/2}$, and $\lambda_\parallel$ of the Fiber Samples Investigated[a]

sample	$\langle R_g^2\rangle^{1/2}$, nm	$\langle R_\perp^2\rangle^{1/2}$, nm	$\lambda_\parallel$ (eq 3)
isotropic	17 ± 0.7	9.8 ± 0.4	
spun, no take-up	16.7 ± 0.7	9.6 ± 0.4	≃1
v_a = 2500 m/min		4.7 ± 0.3	4.4 ± 0.5
v_a = 4000 m/min		4.4 ± 0.3	5 ± 0.5
no take-up and cold-drawn λ = 4		4.5 ± 0.3	4.8 ± 0.5

[a] M_w(PP-*d*) = 10^5 dalton, as determined from the Zimm plot of the isotropic sample.

0.5% and c_D = 1.9% indicate no segregation.

Typical results for the corrected data (for c_D = 1.9%) are shown in Figure 2 for the fibers and an isotropic bulk sample, using the Zimm representation of the intensity, namely,

$$I_\perp(Q)^{-1} = K(1 + Q^2\langle R_\perp^2\rangle) \quad (1)$$

$I_\perp(Q)$ is the intensity measured perpendicular to the fiber axis. $\langle R_\perp^2\rangle$ is the mean-square distance of gyration perpendicular to the fiber axis, where the radius of gyration is given by $\langle R_g^2\rangle = \langle R_\parallel^2\rangle + 2\langle R_\perp^2\rangle$. K is a constant (the data in Figure 2 are not normalized for $I_\perp(0)$). The (unresolved) decay of $I_\parallel(Q)$ with increasing Q is so steep that, also for the lowest Q in Figure 2, the scattered intensity is inside the 22.5° sectors of the area detector from which the $I_\perp(Q)$ data were evaluated. Thus $I_\perp(0)$ is not affected by the integration procedure. (for a detailed discussion of experiments on strongly anisotropic scattering we refer to the paper of Sadler and Barham.[6]) The slope of the straight line in the Zimm plot is interpreted in terms of $\langle R_\perp^2\rangle$, or in terms of $\langle R_g^2\rangle$ for the (nonspun) isotropic sample and the deformed sample without take-up. All results are summarized in Table I.

For the isotropic bulk sample, the extrapolated value of the absolute intensity $I(Q\to 0)$ yields a molecular weight which is M_w = 100 000. For this measurement, the intensity was calibrated by a H_2O scatterer of known transmission, as usually applied at the D 11 instrument in the ILL. For the spun samples, the extrapolated values of $I(Q\to 0)$ do not agree with the value of the isotropic sample. We assume that these discrepancies are caused by the uncertainties of the scattering volumes as mentioned before. We emphasize that the discrepancies are much smaller than those quoted in the experiments of Ballard et al.;[7] these authors give an explanation in terms of the formation of subsections of the molecule.

Considering the values for the radii of gyration in the table, we have to point out that, in spite of the extended linear part of the Zimm plot in Figure 2, eq 1 should only hold for $QR_\perp < 1$ (i.e., for the first three experimental points). The extended Zimm behavior is plausible in view of the observation that, in general, polydispersity tends to increase the apparent range of validity of eq 1 to much higher values of $QR_\perp$ (see, e.g., ref 8,9).

For the undeformed sample, our results can be compared with similar measurements carried out in the range where $R_gQ < 1$.[7,10] Assuming a Schultz distribution of the molecular mass, with $M_w/M_n \simeq 7$, the *z*-average $\langle R_g^2\rangle^{1/2}$ of the radius of gyration listed in Table I can be converted into the mass average by means of the relation $\langle R_w^2\rangle^{1/2} = (2 - M_n/M_w)^{-1/2} \times 17$ nm = 12.5 nm. This is in fairly good agreement with results from the measurements in ref 7 for a quoted "apparent molecular weight" of M_w = 118 000 and a value of $\langle R_w^2\rangle^{1/2}$ = 13.9 nm.

In the following, we interpret our curves in terms of eq 1 and extract a radius of gyration for all samples which were investigated. The conformation of the chain in the deformed state is characterized by the ratios of the radii of gyration $\lambda_\perp$ and $\lambda_\parallel$ defined as

$$\lambda_\perp = (R_\perp/R_g)(3^{1/2}); \qquad \lambda_\parallel = (R_\parallel/R_g)(3^{1/2}) \quad (2)$$

With the hypothesis that the molecules are deformed affinely and that the melt is incompressible ($\lambda_\perp^2\lambda_\parallel = 1$), eq 2 gives

$$\lambda_\parallel = \langle R_{g0}^2\rangle/3\langle R_\perp^2\rangle \quad (3)$$

The last column of Table I with $\lambda_\parallel$ from eq 3 leads to the following conclusions:

(I) In the Q range of our experiments, the molecular elongation $\lambda_\parallel$ of a single chain as determined from the Zimm plots is practically independent of the take-up velocities for v_a = 2500 m/min and 4000 m/min, in spite of the fact that the stress at the solidification point is proportional to v_a^2.

(II) In our experiments for the fast-spun fibers, the molecular elongation of the chains $\lambda_\parallel$ is indentical for samples cold-drawn by a necking process, with a macroscopic deformation λ = 4.

(III) The molecular deformation $\lambda_\parallel$ is approximately equal to the macroscopic deformation λ = 4 for the necking process of the cold-drawn fibers; this is consistent with the assumptions underlying eq 3.

The observed molecular deformation of about 4 means that the single chain has a longitudinal extension L_z of $L_z = 2\lambda_\parallel R_g$ = 136 nm if a rodlike conformation of the chain is assumed. L_z is about $^1/_7$ of the length of the fully extended chain. The long period of the fast spun fibers is 12 nm as determined by us with small-angle X-ray scattering. If one assumes crystalline and amorphous regions forming stacks of lamellae, it follows that a single chain transverses about 11 lamellae in the average.

To estimate the degree of chain folding (the number of tie molecules) it is necessary to evaluate the form factor of the chain parallel to the fiber axis. In order to do so, and to consolidate our first results, the experiment will be continued in particular at smaller Q values. This also allows to judge the hypothesis of affine deformation.

Acknowledgment. We thank Dr. A. Speidel, K. Brakemeier, and N. Michael from Zschimmer & Schwarz GmbH & Co. for the preparation of the fibers and Dr. H. Haberkorn for his X-ray measurements.

Registry No. Neutron, 12586-31-1.

References and Notes

(1) George, H. H.; Holt, A.; Buckley, A. *Polym. Eng. Sci.* **1983**, *23*, 95–99.

(2) Ahmed, M. *Polypropylene Fibers—Science and Technology*; Elsevier: Amsterdam, 1982.
(3) Recent reviews can be found in: *High-Speed Fiber Spinning*; Ziabicki, A., Kawai, H., Eds.; Wiley Interscience: New York, 1985.
(4) Vassilatos, G.; Knox, B. E.; Frankfort, H. R. E. *Dynamics, Structure Development, and Fiber Properties in High-Speed Spinning of Polyethylene Terephthalate*; *High-Speed Fiber Spinning*; Ziabicki, A., Kawai, H., Eds.; Wiley Interscience: New York, 1985.
(5) Ziabicki, A. *Fundamentals of Fiber Formation*; Wiley: New York, 1976.
(6) Sadler, D. M.; Barham, P. J. *J. Polym. Sci., Polym. Phys. Ed.* **1983**, *21*, 309–317.
(7) Ballard, D. G. H.; Burgess, A. N.; Nevin, A.; Cheshire, P.; Longman, G. W.; Schelten, J. *Macromolecules* **1980**, *13*, 677–681.
(8) Ullman, R. *J. Polym. Sci. Polym. Phys. Ed.* **1985**, *23*, 1477–1484.
(9) Beltzung, M.; Picot, C.; Herz, J. *Macromolecules* **1984**, *17*, 663–669.
(10) Ballard, D. G. H.; Longman, G. W.; Crowley, T. L.; Cunningham, A.; Schelten, J. *Polymer* **1979**, *20*, 399–405. Ballard, D. G. H.; Cheshire, P.; Longman, G. W.; Schelten, J. *Polymer* **1978**, *19*, 379–385.

K. Hahn, J. Kerth, and R. Zolk
BASF Aktiengesellschaft
6700 Ludwigshafen, West Germany

D. Schwahn and T. Springer*
Institut für Festkörperforschung
der Kernforschungsanlage Jülich
D-5170 Jülich, Postfach 19 13, West Germany

J. Kugler
Institut Laue-Langevin, Grenoble, France

Received July 20, 1987

Segmental Dynamics in Nylon 66†

Solid-state NMR methods have been of use in elucidating the dynamics of macromolecules at both the segmental[1] and molecular entanglement length scales.[2,3] At the segmental level this approach has been used to characterize the rates and amplitudes of motion, with great molecular specificity, of both completely amorphous[4,5] and semicrystalline[6,7] polymers. In these systems the experimentally determined mechanics of motion have been used to test various theoretical models of segmental motion.[8] There exist a considerable number of models for methylene chains,[9,10] but in these cases it is experimentally difficult to identify individual chain sites and characterize the different types of motion that each methylene group and its neighbors undergo. We present here a preliminary account of the characterization of segmental dynamics of specifically deuteriated nylon 66 polymers (polyhexamethylene adipamide) that allow us to individually identify the molecular motion that each methylene unit undergoes and thus to examine questions as to the cooperativity of motion. Furthermore, this system has the advantage of allowing us to separately examine subsystems of five and seven bonds which are nominally pinned by the hydrogen-bonding amide sites.

We have prepared specifically isotopically labeled nylon 66 polymers by interfacial condensation polymerization of labeled hexamethylene diamine and adipoyl chloride. The polymers are labeled in one chemically distinct position with either deuterium or carbon-13. The as polymerized polymers have a molecular weight distribution which is skewed to low molecular weight; however, a most probable molecular weight distribution is obtained after equilibrating these polymers in the melt. Polymers that have been selectively deuteriated in the diamine moiety at the C_1 and C_6 carbons (NY16NHME), the C_2 and C_5 carbons (NY25NHME), the C_3 and C_4 carbons (NY34NHME) and in the adipoyl moiety at the C_2 and C_5 carbons (NY25COME) and the C_3 and C_4 carbons (NY34COME) are reported on here.

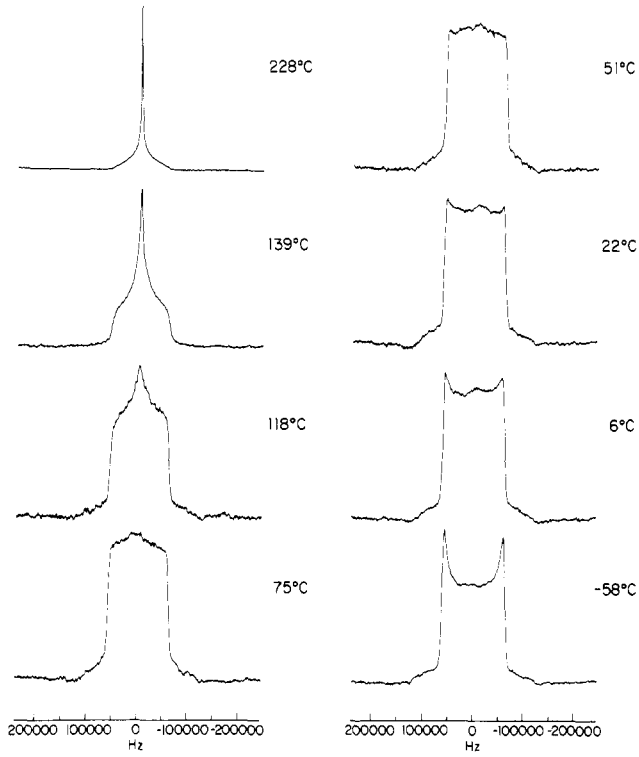

Figure 1. Fully relaxed ^2H NMR spectra at temperatures between −59 °C and 228 °C of nylon 66 that has been selectively deuteriated at the C_1 and C_6 carbons of the diamine moiety.

Figure 1 illustrates temperature-dependent fully relaxed ^2H NMR spectra of nylon 66 polymer labeled with deuterium on the carbons α to the nitrogen. These spectra were obtained with a Bruker MSL-200 NMR spectrometer at a resonance frequency of 30.7 MHz with a quadrupole echo sequence employing a $\pi/2$ radiofrequency pulse length of 2.8 μs and a delay between the quadrature pulses of 20 μs. The spectra are all acquired without symmetrization (no zero filling or data blanking). These spectra contain contributions from both the crystalline and noncrystalline regions of the polymer; however, it is clear that at temperatures above the glass transition temperature (>75 °C at the frequency of this measurement (~100 kHz)) we observe a very narrow component in the line shape which is attributable to methylene groups in noncrystalline domains undergoing essentially isotropic motion that is fast on this time scale. Furthermore, at the lowest temperature illustrated (−58 °C) the spectrum can be approximated as a Pake doublet indicating that we are in the slow-motion limit for all methylene groups α to the nitrogen regardless of the morphology of their environment. These data may be decomposed into components identified with methylene groups in either crystalline or noncrystalline environments by T_1 discrimination experiments; comparison of these results to other measures of crystallinity indicate that the long T_1 component may be quantitatively identified as arising from the crystalline domains and the short T_1 components with the noncrystalline domains. A full line-shape analysis of the decomposed line shapes will be presented in papers to follow.

† Contribution no. 4657.

0024-9297/88/2221-1543$01.50/0